Digest Journal of Nanomaterials and Biostructures Vol. 7, No. 4, October-December 2012, p. 1615-1626

BAND FERROMAGNETISM IN SYSTEMS WITH LINEAR DENSITY OF STATES

G. A. LUNGU, N. G. APOSTOL, M. MORARIU, C. M. TEODORESCU •
National Institute of Materials Physics, P.O. Box MG-7, 077125 Bucharest-Magurele, Romania

The band (or Stoner) ferromagnetism in systems exhibiting a linear density of states, such as a graphene sheet, where the density of states $g(\varepsilon)$ is proportional to ε, is investigated as function of temperature. The calculations are performed by neglecting spin-wave excitations and some arguments are presented for this approximation. It is found that the occurrence of ferromagnetism becomes easier at finite temperature than in the low temperature limit, especially for systems with low values of carrier density. An almost linear dependence of the magnetization on temperature is predicted; the temperature of vanishing magnetization is linear with the value of the equilibrium Fermi energy, irrespective of the value of the interaction (Hubbard) parameter. Also, for low values of the Hubbard energy an increase in the average value of the polarization with the temperature is predicted in the range of low temperatures. The most important application of such systems consists of control over the onset of magnetization by the charge density (the value of the Fermi energy).

(Received October 11, 2012; Accepted October 16, 2012)

Keywords: band ferromagnetism, Stoner criterion, graphene, carrier-controlled magnetism

1. Introduction

The prototype of a system with linear density of states (DOS) is given by infinite graphene sheets, where the energy around the K point in the Brillouin zone is linear in the absolute value of the wave vector $\varepsilon(k) \sim k \sim (k_x^2 + k_y^2)^{1/2}$, which is sometimes called a 'Dirac spectrum' [1]. Therefore, the two-dimensional sum over the states isolates a factor k in the integral over the absolute value of the wavevector, and this is proportional to the energy. The dependence $\varepsilon = \hbar c' k$ involves a pseudo-speed of light (or a Fermi velocity) $c' \approx 10^6$ m/s [1].

Ferromagnetism in graphenes has been the subject of an increasing amount of work during the last years, although its origins are still subject to intensive debates [2]. The occurrence of ferromagnetism is usually associated with boundary effects [3] or with the occurrence of a spin polarized flat band [1,4]. The pure Stoner ferromagnetism of graphenes was accounted for only recently [5], with the prediction of a continuous quantum magnetic phase transition (Stoner phase). Bilayers of graphene have also been predicted to exhibit ferromagnetism in the low density regime, with lower interaction energies U as compared to the usual Stoner criterion [6]. Doping, even with nonmagnetic impurities, leads in some cases to magnetic ordering [7]. The sound experimental discovery of room temperature ferromagnetism in graphenes [8,9] and in irradiated graphite [10] is expected to boost this research even more. However, to date, most of the theoretical work explained the possible occurrence of ferromagnetism through edge states [3,4] or via spin-polarized or -unpolarized defects (vacancies) [7,11], although Ref. [9] suggest a possible intrinsic mechanism of ferromagnetic ordering. Also, recently, a Hubbard model for graphene was proposed [c], though without any eventual connection to a Stoner criterion. In this work, we will start by assuming the validity of the Hubbard mechanism from Ref. [12] and, based on this approach, we will develop a phenomenological approach aiming to sketch a simple variable-

•Corresponding author: teodorescu@infim.ro

temperature Stoner theory of the ferromagnetism in systems where the DOS is linear with the energy, of which graphenes are the most straightforward example.

A rather didactical introduction in the band ferromagnetism and its connections with the dimensionality of the system and with the Hubbard model was presented in [13]. In the following, we will follow the path traced in Ref. [14]: first we compute the zero temperature properties of the system (Sec. 2), then the density and the position of Fermi energies for the case of finite temperature (Sec. 3), the energy of the system (Sec. 4), the stability of the ferromagnetic phase (Sec. 5), and the average value of the polarization and its dependence with the temperature (Sec. 6).

It may be argued that in a first approximation the spin wave excitations in two dimensional (2D) systems present a long wavelength divergence and may lead to the destruction of ferromagnetism. In Sec. 7, we also present a short review of surface spin wave theories and recent experiments, and argue that, in a first approximation, it is not straightforward that this destruction manifests. Therefore, neglecting spin waves in the present theory might provide a good approximation for the description of pure 2D Stoner systems. Finally, in Sec. 8 we draw the main conclusions of this paper.

Throughout this paper, we shall consider only unbalanced carriers (electrons or holes). We consider that neutral graphene has completely filled valence band and completely empty conduction band. All densities discussed in the following concern only carriers obtained by doping or by injection from external sources, including charging of the graphene sheet. The linear energy-dependent DOS is expressed as:

$$g(\varepsilon) = \frac{n\varepsilon}{{\varepsilon_F}^{(0)2}}, \qquad \text{such as, at } T = 0: \int_0^{\varepsilon_F^{(0)}} g(\varepsilon)d\varepsilon = \frac{n}{2}, \tag{1}$$

n being the conduction (doped) electron density (per unit area), and $n/2$ the doped electron density of one subband (spin ↑ or ↓) in the absence of polarization. In the presence of a band polarization ξ, $n\xi/2$ electrons are promoted from the subband ↓ to the subband ↑; therefore, the Fermi energies corresponding to both subbands are shifted such that:

$${\varepsilon_F}^{\uparrow,\downarrow}(0) = {\varepsilon_F}^{(0)}\left(1 \pm \xi\right)^{1/2} \tag{2}$$

We now estimate the order of magnitude of the Fermi energy and of the carrier density. From the formula $\varepsilon = \hbar c'k$ one estimates that the connection between the Fermi energy and the doped carrier density is $n = (1/4\pi)\,[\varepsilon_F^{(0)}/(hc')]^2$. Therefore, if one assumes that each atom in the lattice contributes with δ electrons (or holes) to the carrier density, we obtain $\varepsilon_F^{(0)} \approx 92.8$ eV $\delta^{1/2}$. A possible doping may also be accounted for by this estimate: for instance, a doping of 10^{-6} induces a Fermi energy of 92.8 meV, which approaches the thermal energy corresponding to room temperature.

2. The zero temperature case. The Stoner criterion

The two basic hypotheses of the calculation are the following:

(i) Near the graphene's K point, the dispersion law is linear. This is a consequence of the band structure of graphene, obtained just from tight binding theory [15] without taking into consideration the Hubbard interaction [12]. More complicated dispersion laws may be derived (see e.g. Ref. [16]) by including the Hubbard interaction in a more sophisticated theory such as random phase approximation (RPA), but in the following we will just consider the main result of the tight binding model $\varepsilon(k) \sim k$ plus the Hubbard interaction taken in the mean field approximation.

(ii) The band ferromagnetism is treated in the rigid band displacement model.

In the case of spin polarization, an increase occurs in the kinetic energy, compensated by the Hubbard term - $nU\xi^2/4$ for all electrons in the area of unity [13]. The increase in the kinetic energy is obtained simply by integrating $\varepsilon g(\varepsilon)$ over both subbands ↑ and ↓, with subsequent subtraction of the energy of unpolarized subbands. The energy variation induced by the occurrence of the spin polarization ξ is obtained as:

$$\Delta w(\xi) = n\varepsilon_F^{(0)} \left\{ \frac{(1+\xi)^{3/2} + (1-\xi)^{3/2} - 2}{3} - \frac{u\xi^2}{4} \right\} \tag{3}$$

where $u = U / \varepsilon_F^{(0)}$. The first term of the total energy per unit area is quite similar to the leading term (at low densities) of the Hartree-Fock energy from the model of zero-temperature two-dimensional electron gas discussed by Tanatar and Ceperley two decades ago [17]. Typical energy curves $\Delta w(\xi)$ are represented in Figure 1. Three regions may be defined, as a function of the parameter u, reflecting the ratio between the Hubbard energy and the zero temperature Fermi energy: (i) for $u < 1$, the absolute minimum of the energy curves is the paramagnetic state $\xi = 0$; (ii) for $1 \le u < \sqrt{2}$ there occurs a minimum energy for $\xi \neq 0$, namely for $\xi = 2(u^2 - 1)^{1/2}/u^2$; (iii) for $u \ge \sqrt{2}$ the most stable state is the ferromagnetic one, with maximum polarization $\xi = 1$. One may also easily verify the fulfilment of the Stoner criterion for the magnetic instability $g(\varepsilon_F^{(0)})U > n$: the condition of instability for the paramagnetic phase $(\partial \Delta w/\partial x)_{\xi=0} < 0$ implies $u > 1$.

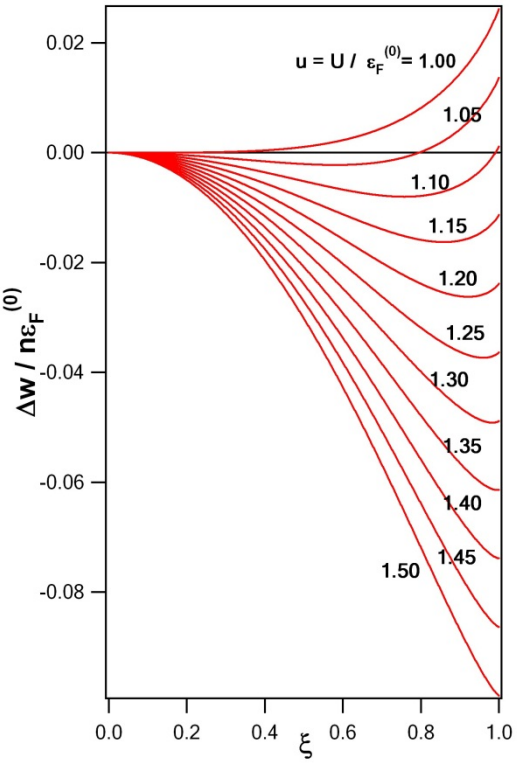

Fig. 1. Energy dependence at T = 0 on the asymmetry parameter, for several values of the ratio between the Hubbard and the equilibrium unpolarized Fermi energy.

3. The finite temperature case. Position of Fermi energies

In the absence of polarization at finite temperature, eq. (1) is rewritten by introducing the Fermi-Dirac distribution:

$$\int_0^{\infty} \frac{g(\varepsilon)d\varepsilon}{\exp\left[\dfrac{\varepsilon-\varepsilon_F(T)}{k_B T}\right]+1} = \frac{n}{2} \tag{4}$$

With notations $y_0 = \varepsilon_F^{(0)} / (k_B T)$; $y = \varepsilon_F(T) / (k_B T)$; $x = \varepsilon / (k_B T)$:

$$\int_0^{\infty} \frac{x dx}{\exp(x-y)+1} = \frac{1}{2}\left\{x^2 - 2x\ln\left[\exp(x-y)+1\right] - 2\mathrm{Li}_2\left[-\exp(x-y)\right]\right\}_0^{\infty} = \frac{{y_0}^2}{2} \tag{5}$$

(see Ref. [14]) where $\mathrm{Li}_2(z)$ is the dilogarithm function. The polylogarithm function is defined as [14,18]:

$$\mathrm{Li}_n(z) = \sum_{j=1}^{\infty} \frac{z^j}{j^n} = \int_0^z \frac{\mathrm{Li}_{n-1}(t)}{t} dt \tag{6}$$

In evaluating the right-hand side term of eq. (5), the Landen identity is used [15], written as:

$$\mathrm{Li}_2\left(-\exp(x-y)\right) = -\mathrm{Li}_2\left(\left[\exp(y-x)+1\right]^{-1}\right) - \frac{1}{2}\left[\ln\left(1+\exp(x-y)\right)\right]^2 \tag{7}$$

together with $\mathrm{Li}_2(1) = \pi^2/6$. Finally, eq. (5) yields:

$$y^2 + 2\mathrm{Li}_2\left(-\exp(-y)\right) + \frac{\pi^2}{3} = {y_0}^2 \tag{8}$$

Eq. (8) is represented in Figure 2. An important observation is that the Fermi energy at finite temperature has a nonzero value only for $y_0 > 6^{-1/2}\,\pi \approx 1.282$ (or $\varepsilon_F^{(0)} > 6^{-1/2}\,\pi\, k_B T \approx 1.283\, k_B T$). [Note that $\mathrm{Li}_2(-1) = -\pi^2/12$.] Otherwise, the system is an insulator, with no free electrons. A similar result was obtained in Ref. [14] for a constant DOS, where a nonzero Fermi energy occurs at finite temperature only for $\varepsilon_F^{(0)} > \ln 2\, k_B T \approx 0.693\, k_B T$. This implies that such systems, where $\varepsilon_F^{(0)}$ has a small value (in the range of 1-100 meV) are conductive at low temperatures and insulating at higher temperatures, with the transition temperature given by $k_B T_0 = (\ln 2)^{-1} \varepsilon_F^{(0)}$ in the case of a constant DOS and, respectively, $(6^{1/2}\pi^{-1})\, \varepsilon_F^{(0)}$ in the case of a linear DOS. The transition temperature is almost two times lower in the case of a linear DOS than in the case of a constant DOS, for the same value of the zero temperature Fermi energy.

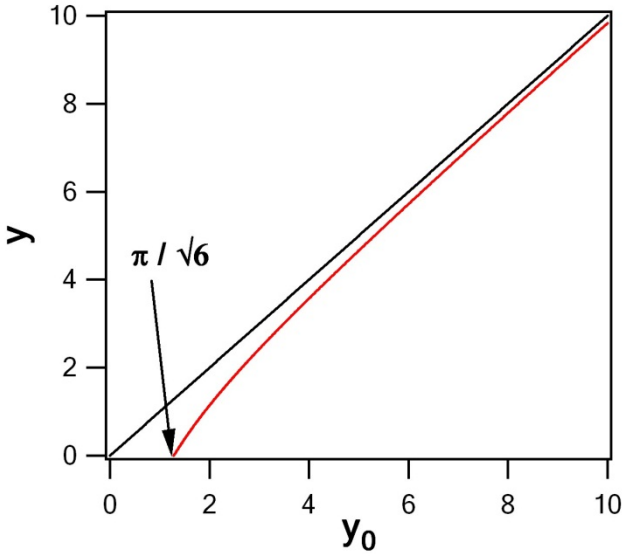

Fig. 2. The dependence $y(y_0)$ represented by eq. (8).

Also, the dependence $y \equiv \alpha(y_0)$ from eq. (8) may be well approximated with the following rational function, in the range $6^{-1/2}\,\pi < y_0 < 10$:

$$\alpha(y_0) \approx \frac{y_0^{\,2} + 0.16753 y_0 - 1.8761}{y_0 + 0.14407} \approx y_0 - \frac{\pi^2}{6 y_0} \tag{9}$$

the errors being in the range of 0.5 %.

Eq. (8) may be generalized also for the spin-polarized subbands, with the notations: $y_\uparrow = \varepsilon_F^{\uparrow}(T) / (k_B T)$ and $y_\downarrow = \varepsilon_F^{\downarrow}(T) / (k_B T)$:

$$y_\uparrow^{\,2} + 2\mathrm{Li}_2\big(-\exp(-y_\uparrow)\big) + \frac{\pi^2}{3} = y_0^{\,2}(1+\xi) \tag{10a}$$

$$y_\downarrow^{\,2} + 2\mathrm{Li}_2\big(-\exp(-y_\downarrow)\big) + \frac{\pi^2}{3} = y_0^{\,2}(1-\xi) \tag{10b}$$

By using the approximation given by eq. (9), the Fermi energies of the spin polarized subbands are given by:

$$y_{\uparrow,\downarrow} = \alpha\big(y_0(1 \pm \xi)^{1/2}\big) \tag{11}$$

An important consequence of the fact that a nonzero Fermi energy at finite temperature exists only for a minimum value of the zero temperature Fermi energy is that, from eq. (10b), a maximum value of the polarization is allowed, such that $y_0(1 - \xi_{max})^{1/2} = 6^{-1/2}\,\xi$. From here, the maximum allowed polarization is found to be $\xi_{max} = 1 - \pi^2/(6\,y_0^{\,2})$. This correspunds to $y_\downarrow(\xi_{max}) = 0$.

4. The finite temperature case. The total energy of the system

For a subband indexed by $s = +1(\uparrow)$ or $s = -1\ (\downarrow)$, its kinetic energy is given by:

$$\varepsilon_s = \int_0^\infty \frac{\varepsilon g(\varepsilon) d\varepsilon}{\exp\left[\dfrac{\varepsilon - \varepsilon_F^{\,s}(T)}{k_B T}\right] + 1}, \text{ implying } \frac{\varepsilon_s}{n k_B T} = \frac{1}{y_0^{\,2}} \int_0^\infty \frac{x^2 dx}{\exp(x - y_s) + 1} \tag{12}$$

The primitive in the right-hand side, as computed by Wolfram Mathematica [19], is given by:

$$\frac{1}{3}\Big\{-6x\mathrm{Li}_2\big(-\exp(x-y)\big) + 6\mathrm{Li}_3\big(-\exp(x-y)\big) + x^2\big[x - 3\ln\big(\exp(x-y)+1\big)\big]\Big\} \tag{13}$$

When computing the $x \to \infty$ limit, one uses the Landen identity (7) for Li_2, together with the following identity for Li_3 [20]:

$$\mathrm{Li}_3(-z^{-1}) - \mathrm{Li}_3(-z) = \frac{(\ln z)^3}{6} + \frac{\pi^2}{6}\ln z \tag{14}$$

After some algebra, the definite integral from eq. (12) is evaluated as:

$$\int_0^\infty \frac{x^2 dx}{\exp(x - y_s) + 1} = \frac{y_s^{\,3}}{3} + \frac{\pi^2 y_s}{3} - 2\mathrm{Li}_3\big(-\exp(-y_s)\big) \equiv \beta(y_s) \tag{15}$$

The function $\beta(y_s)$ is represented in Figure 3. For $0 \le y_s < 10$, the function β may be approximated as:

$$\beta(y_s) \approx \frac{y_s^{\,3}}{3} + \frac{\pi^2 y_s}{3} + 1.8205\exp(-0.9561 y_s) \tag{16}$$

with errors lower than 0.6 %.

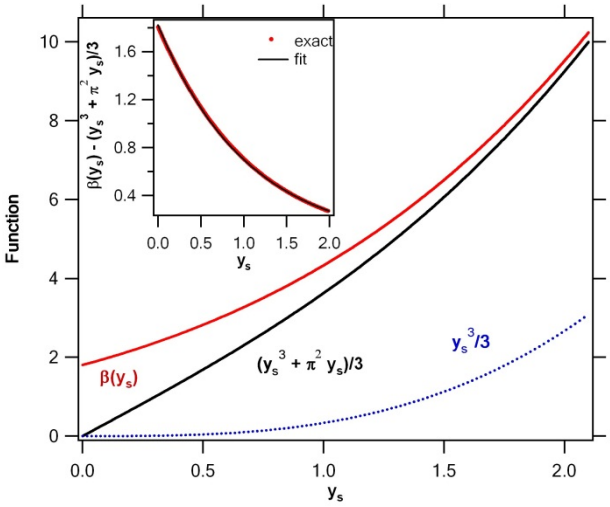

Fig. 3. The dependence $\beta(y_s)$ given by the expression of the energy integral - eq. (15), together with the case of zero temperature (blue dotted curve) and only the first terms of eq. (15), without the polylogarithm function. Insert: exponential decay fitting of the polylogarithm function.

Let us remark that there is a strong departure of the energy as a function of y_s with respect to the zero temperature case, where the energy integral is simply proportional to $y_s^{\,3}/3$ (dashed curve in Figure 3).

Thus, one may easily compute the total energy of the system, by summing the total kinetic energy $\varepsilon_\uparrow$ and $\varepsilon_\downarrow$ with the Hubbard energy - (1/4) $nU\xi^2$. The kinetic energy of the unpolarized system is subtracted from this energy, which yields the stabilization energy of the ferromagnetic phase Δw:

$$\omega(u', y_0, \xi) \equiv \frac{\Delta w}{n k_B T} =$$

$$= \frac{1}{y_0^{\,2}}\left\{\frac{y_\uparrow^{\,3} + y_\downarrow^{\,3} - 2y^3}{3} + \frac{\pi^2}{3}\left(y_\uparrow + y_\downarrow - 2y\right) - 2\left[\mathrm{Li}_3(-e^{-y_\uparrow}) + \mathrm{Li}_3(-e^{-y_\uparrow}) - 2\mathrm{Li}_3(-e^{-y})\right]\right\} - \frac{u'\xi^2}{4} \tag{17}$$

where $u' = U / (k_B T)$. $y_\uparrow(T, \xi)$, $y_\downarrow(T, \xi)$ and $y(T)$ are given by eqs. (8) and (10). Alternatively, using the approximated functions α and β defined by eqs. (9) and (16), the ferromagnetic energy may be written as:

$$\omega(u', y_0, \xi) = \frac{\Delta w}{n k_B T} = \frac{1}{y_0^{\,2}}\left\{\beta\left[\alpha\left(y_0(1+\xi)^{1/2}\right)\right] + \beta\left[\alpha\left(y_0(1-\xi)^{1/2}\right)\right] - 2\beta\left[\alpha(y_0)\right]\right\} - \frac{u\xi^2}{4} \tag{18}$$

Three dimensional plots of $\omega(u', y_0, \xi)$ are given in Figure 4 for two values of $u' = U / (k_B T)$. One may remark that at low Hubbard parameter and low value of the equilibrium zero temperature Fermi level the paramagnetic state is the most stable. For low Hubbard parameter (Figure 4a), one needs a further increase of the zero temperature Fermi level value (or, alternatively, a decrease in temperature) in order to obtain the stability of the ferromagnetic state. For higher values of the Hubbard parameter (Figure 4b), the most stable state is the ferromagnetic state even for the lowest allowed value of $y_0 = 6^{-1/2}\,\pi$.

In the following, we investigate in detail the conditions where the ferromagnetic state is stable.

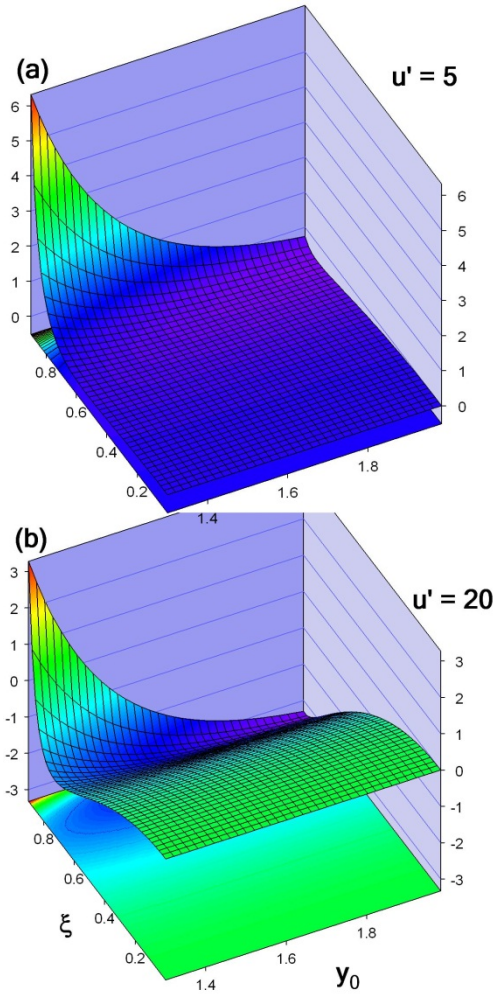

Fig. 4. Energy surface plots as function on the normalized Fermi energy $y_0 = \varepsilon_F^{(0)} / (k_B T)$ and asymmetry parameter ξ, for two values of the normalized Hubbard energy $u' = U / (k_B T)$.

5. Stability of the ferromagnetic phase

From the energy given by eqs. (17-18) the extremum condition $\partial\omega/\partial\xi = 0$ yields, after some algebra:

$$u = \frac{u'}{y_0} = \frac{U}{\varepsilon_F^{(0)}} = \frac{y_0\left(\frac{1}{\xi}+1\right)}{y_\uparrow + \ln\left(1+e^{-y_\uparrow}\right)} - \frac{y_0\left(\frac{1}{\xi}-1\right)}{y_\downarrow + \ln\left(1+e^{-y_\downarrow}\right)} \equiv a(y_0,\xi) \qquad (19)$$

Plots of the function $a(y_0, \xi)$ are represented in Figure 5, where the curve indicating the ξ_{max} limitation [$\xi_{max} = 1 - \pi^2/(6\, y_0^2)$] is given as well. For a given value of the parameter y_0 one may represent a horizontal line at ordinate $y = u$ on the corresponding curve from Figure 5. If this line intersects the curve $a(y_0, \xi)$, the point of intersection represents the equilibrium value of the polarization ξ_0 (if $\xi_0 < \xi_{max}$). If there is no intersection, i.e. the line corresponding to u lies always above the corresponding curve $a(y_0, \xi)$, the energy curve is concave as a function of ξ over the whole allowed interval of polarizations, and thus the system evolves in the state of maximum allowed polarization ξ_{max}. Conversely, if the horizontal $y = u$ line lies below $a(y_0, \xi)$, the energy

curve is convex over the whole interval and the system has its equilibrium state at $\xi = 0$, i.e. in the paramagnetic state.

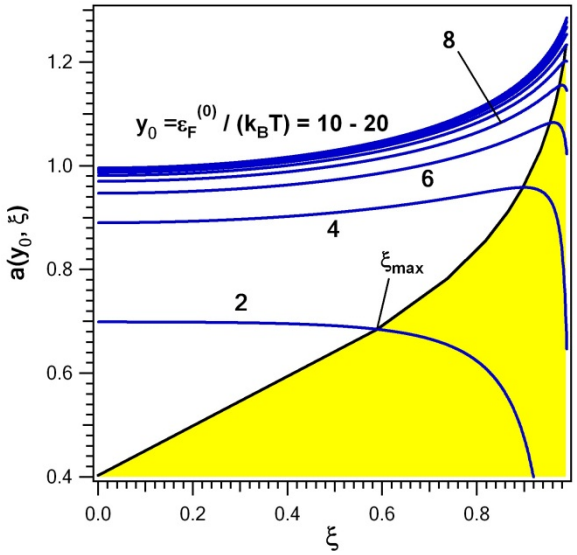

Fig. 5. Plots of the function $a(y_0,\xi)$, resulted from the derivative of the total energy. The intersections of these curves with horizontal lines $y = u$ yield positions of the energy minima at nonvanishing polarization. The yellow region represents the area of forbidden polarization values.

The ferromagnetic state is sometimes, especially for low values of y_0, achievable for lower ratios between the Hubbard and the Fermi energies in the case of finite temperature than in the case of zero temperature (let us recall the zero temperature Stoner criterion $u > 1$). This result is in line with the result obtained in Ref. [6] for bilayer graphenes, but with simpler considerations in this case; also, according to the present phenomenological theory, this property is intrinsic to the system under consideration and follows only from the supposition regarding the density of states, whereas in Ref. [6] it was a consequence of both graphene structure through tight binding ingredients, and of other phenomena taken into account by the proposed model, such as hopping between planes. The actual computation explains better the recent experimental data on undoped graphene from Ref. [9].

6. The temperature dependence of average polarization

In view of the above paragraph, the strongest deviations from the zero-temperature Stoner criterion are expected for low values of $y_0 = \varepsilon_F^{(0)} / k_B T$. In this range, one may expect the following unusual magnetic behaviour: suppose that the ration between the Hubbard and the Fermi energies u is such that the system is paramagnetic at a given temperature T_1, corresponding to a given dimensionless parameter y_{01}. In terms of eq. (19), $u < a(y_{01}, \xi)$ for all allowed ξ values in the range $(0, \xi_{max})$. When the temperature is increased at $T_2 > T_1$, the parameter y_0 decreases to $y_{02} < y_{01}$, such that it might be possible that the new curve $a(y_{02}, \xi)$ starts to intersect the line $y = u$ or even $u > a(y_{02}, \xi)$ for the whole range of allowed ξs. That is, such a system becomes ferromagnetic when the temperature is increased. A similar behaviour was already demonstrated for a constant DOS in Ref. [14].

However, such behaviour is observed when both the equilibrium Fermi energy and the Hubbard energy are on the order of magnitude of the thermal energy $k_B T$. In such cases, thermal fluctuations are important and it makes sense to compute an average polarization fraction, defined as [14]:

$$< \xi >= \frac{\int_0^{\xi_{max}} \xi \exp[-\omega(u, y_0, \xi)] d\xi}{\int_0^{\xi_{max}} \exp[-\omega(u, y_0, \xi)] d\xi} \tag{20}$$

The result of this computation is represented in Figure 6. This has to be compared with Figure 5b from Ref. [14]. The general behaviour is generally the same: the resulting magnetization curves $M(T)$ exhibit an almost linear decrease with the temperature. Such magnetization curves were already reported so far for magnetic surfaces [21,22] but at this stage it is difficult to connect this experimental behaviour to the case presented here of a linear DOS or to the case analyzed previously of a constant DOS [14]. Let us just remark that in the case of Ni monolayers deposited on Cu(001) [21], the present model might be appropriate in terms of 3*d holes*, since the Fermi energy lies very close to the 3*d* band maximum [24].

As in the case of a constant DOS [14], at low values of $u = U / \varepsilon_F^{(0)}$ (≈ 0.5) an increase of the magnetization with the temperature at low temperatures is predicted; $M(T)$ shows a maximum and then it starts to decrease. Such behaviour could be expected from the curves represented in Figure 5. At these low values of u, the most stable microscopic state is the paramagnetic one $u < a(y_0, \xi)$, but the relative stability of the paramagnetic state is on the order of the thermal energy; therefore, states with nonvanishing polarization may be realized and the average via the integral represented by eq. (20) yields a nonvanishing value; however, this average value decreases when the difference between $a(y_0, \xi)$ and u increases, i.e. for smaller values of T (or larger y_0 values).

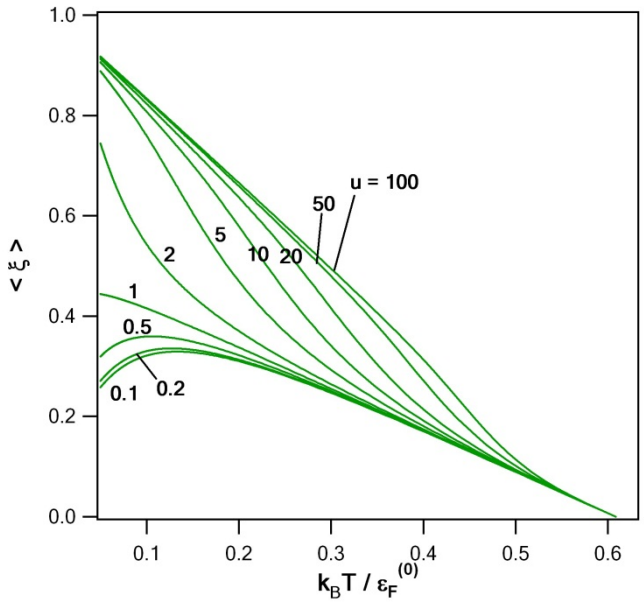

Fig. 6. Temperature dependence of the average polarization, resulted from eq. (20).

Another important result obtained in this case is that the temperature of vanishing average polarization shows an almost linear dependence with the value of the equilibrium Fermi energy: $T_0 \approx 0.6\ \varepsilon_F^{(0)} / k_B$, irrespective of the value of the interaction (Hubbard) parameter. Therefore, in this temperature range close to the dissapearance of magnetism, doping affects the magnetic behaviour of the system in a predictable way. Suppose, for instance, that the system is engineered such that near the room temperature (T_R) the condition $k_B T_R / \varepsilon_F^{(0)} \approx 0.6$ is fulfilled. Thus, any depletion of the charge carriers (e.g. by photoelectric effect or by injection of carriers of opposite sign) will induce ferromagnetism in the system. Conversely, an enrichment of the charge density of a ferromagnetic system may lead to the dissapearance of magnetism. Let us emphasize once more that this finding is not dependent on the value of the Hubbard energy; this energy influences only the magnitude of the average value of the low temperature magnetization.

7. Arguments for neglecting spin waves

The classical Heisenberg spin wave theory [24] stipulates that the decrease of the magnetization with temperature is expressed in terms of the sum over the magnon states $\boldsymbol{k}$, such that $|\Delta M(T)|/M(0) \sim \sum_{\boldsymbol{k}} n_{\boldsymbol{k}}$, where, in 2D systems:

$$\sum_k n_k \propto \int_0^\infty \frac{kdk}{\exp\left[\omega(k)/k_B T\right]-1} \tag{21}$$

with $\omega(k)$ being the magnon energy dependence on the wavevector (or the dispersion law). It is clear that a quadratic dependence $\omega(k) \sim k^2$ induces a logarithmic divergence at high magnon wavelengths and this causes instantaneous destruction of the net magnetisation for any finite temperature. This can be connected also to the Mermin-Wagner theorem [25], which stipulates that no long range magnetic order occurs for infinite, isotropic 2D Heisenberg spin systems. However, there are several limitations to the extrapolation of this theory of localized (Heisenberg) spin systems to Stoner (itinerant) spin systems.

This adaptation, evidencing a spin-wave-like excitation spectrum through quantum field theory applied to the continuous ferromagnetic system, was drawn several decades ago by Herring and Kittel [26]. Many results of this early theory, however, are valid only for long magnon wavelengths. Moreover, by including anisotropy, the magnon dispersion law is simulated by $\omega(k) \sim A + B \times k$ rather than by a quadratic law (see Figure 1 from [25]) and for this condition the integral (21) doesn't diverge anymore. After some decades, Griffin and Gumbs [27] evidenced a surface magnon mode that remains finite and very large at vanishing k. This result was criticised by Mathon [28] for the lack of satisfying spin-rotational invariance. Nevertheless, a newer random phase approximation (RPA) theory [29], which took into account Mathon's criticism, still predicted a magnon dispersion for slabs of a few layers of the type $\omega(k) \sim A + B \times k^2$, which still could not induce any divergence in the sum over magnon states (21). This theory was further developed [30] to provide magnon dispersion laws with non vanishing ω when $k \rightarrow 0$ (Figure 7 from [30]). Also, in Ref. [30] a similarity was reported with a Heisenberg system where next-nearest neighbor interaction is taken into account instead of a simple system with only nearest-neighbor interaction. Therefore, at this point, a complete theoretical similarity with the basic textbook Heisenberg spin system is questionable.

Alternatively, even though a quadratic magnon dispersion law is to be taken into account, the finite sample size may induce a cutoff [the integral in (21) is not taken from 0] in the long magnon wavelength regime, which may stabilise the ferromagnetism in ultrathin layers, as was evidenced both theoretically and experimentally in Ref. [21].

Recent outstanding spin-resolved electron energy loss spectroscopy (SPEELS) experiments on a few single atomic magnetic Co layers [31-32] did not provide relevant data for the spin wave dispersion law around $k = 0$. The data presented in Ref. [31] in this small k region are neutron inelastic scattering data for a Co:(8 % Fe) bulk alloy.

As a summary, there is still no definite theory or clear experimental evidence of a quadratic (or more drastic, $\omega \sim k^n$, $n > 2$, no offset) magnon dispersion law which might definitely suppress the ferromagnetism in a 2D system via a divergence in the sum over magnon states (21).

Therefore, in the present paper it might be a reasonable first approach to neglect spin waves in order to assess ferromagnetism in graphene or other Dirac-like systems only based on very simple Stoner theory considerations. Nevertheless, the incorporation of spin waves into the present treatment is an appealing possible continuation of the present work.

8. Conclusions

This work presents a simple, phenomenological temperature dependent theory of band (Stoner) ferromagnetism for systems where the density of states has a linear dependence on the energy, with special applications to the case of graphene ferromagnetism. This work is a natural expansion of previous Hubbard computations [12], where the occurence of the ferromagnetic ordering is connected to the Stoner criterion. Additionally, at low temperatures, the Stoner

criterion may be diveded into two subcriteria, one for $n \le g(\varepsilon_F^{(0)})U < n\sqrt{2}$ where a ferromagnetic state is stabilized for a nonzero polarization $\xi < 1$, the other one for $g(\varepsilon_F^{(0)})U \ge n\sqrt{2}$, where the most stable state is the ferromagnetic one, with maximum polarization $\xi = 1$.

The main results of the nonzero temperature study are: (i) At finite temperature and low values of the Fermi energy, the ferromagnetism occured for a more relaxed condition (i.e. for lower values of the Hubbard parameter) than the Stoner criterion at zero temperature. This is in line with previous predictions [3], but in this case this finding is derived from a pure phenomenological theory, without involving edge states or defects. (ii) At low temperatures and low values of the Hubbard parameter, an increase in the magnetization with temperature is predicted: $\partial M/\partial T > 0$. A similar behaviour is reported in Ref. [14] for constant density of states. We did not yet find an experimental of such behaviour in pure graphenes, although in Ref. [12] it seems that, when one subtracts the paramagnetic component from the 2 K hysteresis loop, a smaller magnetization remains for one of the two samples investigated, as compared with the 300 K case. (iii) A general trend of the magnetization dependence with temperature is an almost linear dependence. Zero magnetization is achieved at almost constant $\varepsilon_F^{(0)}/k_B T \approx 0.6$, irrespective of the value of the interaction (Hubbard) parameter U.

Acknowledgements: This work is supported by the Romanian National Authority for Scientific Research under the contract PCCE ID_76/2009.

References

[1] B. Partoens, F.M. Peeters, Phys. Rev. **B 74**, 075404 (2006).
[2] R.R. Nair, M. Sepioni, I-Ling Tsai, O. Lehtinen, J. Keinonen, A. V. Krasheninnikov, T. Thomson, A.K. Geim, I. V. Grigorieva, Nature Physics **8**, 199 (2012).
[3] K. Kusakabe, M. Maruyama, Phys. Rev. **B 67**, 092406 (2003).
[4] X. Yang, G. Wu, ACS Nano **3**, 1646-1650 (2009); K. Kusakabe, M. Maruyama, S. Tsuneyuki, K. Akagi, Y. Yoshimoto, J. Yamaguchi, J. Magn. Magn. Mater**. 272**, E737-E738 (2004).
[5] A. Qaiumzadeh, R. Asgari, Phys. Rev. **B 80**, 035429 (2009).
[6] E.V. Castro, N.M.R. Peres, T. Stauber, N.A.P. Silva, Phys. Rev. Lett. **100**, 186803 (2008).
[7] H. Kumazaki, D.S. Hirashima, J. Phys. Soc. Jpn. **76**, 064713 (2007); H. Kumazaki, D.S. Hirashima, J. Magn. Magn. Mater. **310**, 2256-2258 (2007).
[8] Y. Wang, Y. Huang, Y. Song, X. Zhang, Y. Ma, J. Liang, Y. Chen, Nano Lett. **9**, 220 (2009).
[9] Y. Wang, Y. Huang, Y. Song, X. Zhang, Y. Ma, J. Liang, Y. Chen, Nano Lett. **9**, 220-224 (2009).
[10] P. Esquinazi, A. Setzer, R. Höhne, C. Semmelhack, Y. Kopelevich, D. Spemann, T. Butz, B. Kohlstrunk, M. Lösche, Phys. Rev. **B 66**, 024429 (2002).
[11] P.O. Lehtinen, A.S. Foster, Y. Ma, A.V. Krasheninnikov, R.M. Nieminen, Phys. Rev. Lett. **93**, 187202 (2004); O.V. Yazyev, L. Helm, Phys. Rev. **B 75**, 125408 (2007).
[12] T. Ma, F. Hu, Z.B. Huang, H.Q. Lin, Appl. Phys. Lett. **97**, 112504 (2010).
[13] C.M. Teodorescu, G.A. Lungu, J. Optoelectron. Adv. Mater. **10**, 3058-3068 (2008).
[14] G.A. Lungu, C.M. Teodorescu, J. Optoelectron. Adv. Mater. **11**, 369-379 (2009).
[15] P.R. Wallace, Phys. Rev. Lett. **71**, 622-634 (1947); J.C. Slonczewski, P.R. Weiss, Phys. Rev. **109**, 272-279 (1958); G.W. Semenoff, Phys. Rev. Lett. **53**, 2449-2452 (1984).
[16] N.M.R. Peres, M.A.N. Araujo, D. Bozi, Phys. Rev. **B 70**, 195122 (2004).
[17] B. Tanatar, D.M. Ceperley, Phys. Rev. **B 39**, 5005 (1989).
[18] M. Abramowitz, I.A. Stegun, *Handbook of Mathematical Functions with Formulas, Graphs, and Mathematical Tables*, Dover, New York, 1999.
[19] http://integrals.wolfram.com (accessed 15/12/2010)
[20] http://functions.wolfram.com/ZetaFunctionsandPolylogarithms/PolyLog/17/ShowAll.html (accessed 15/12/2010)
[21] C.M. Teodorescu, Surf. Sci. **601**, 4292-4296 (2007).

[22] Y. Huttel, C.M. Teodorescu, F. Bertran, G. Krill, Phys. Rev. **B 64**, 094405 (2001); C.M. Teodorescu, M.C. Richter, K. Hricovini, J. Optoelectron. Adv. Mater**. 8**, 1200-1205 (2006).
[23] J.C. Slater, Phys. Rev. **49**, 537-545 (1936); T. Greber, T.J. Kreutz, J. Osterwalder, Phys. Rev. Lett. **79**, 4465-4468 (1997).
[24] Kittel C, *Introduction to solid state physics*, 4th ed., Wiley, New York, 1971.
[25] N.D. Mermin, H. Wagner, Phys. Rev. Lett. **17**, 1133-1136 (1966).
[26] C. Herring, C. Kittel, Phys. Rev. **81**, 869-880 (1951).
[27] A. Griffin, G. Gumbs, Phys. Rev. Lett. **37**, 371-375 (1976).
[28] J. Mathon, Phys. Rev. **B 24**, 6588-6595 (1981).
[29] M.P. Gokhale, D.L. Mills, Phys. Rev. **B 49,** 3880-3893 (1994).
[30] M. Plihdal, D.L. Mills, Phys. Rev. **B 52**, 12813-12828 (1995).
[31] R. Vollmer R, M. Etzkorn, P.S. Anil Kumar, H. Ibach, J. Kirschner, Phys. Rev. **Lett. 91**, 147201 (2003).
[32] M. Etzkorn, P.S. Anil Kumar, W. Tang, Y. Zhang, J. Kirschner, Phys. Rev. **B 72**, 184420 (2005).